Title page

Full title

2d-PIC simulation of atomic clusters in intense laser fields

Authors

F. Greschik and H.-J. Kull,

Institut für Theoretische Physik A, RWTH Aachen, Germany

Corresponding author and reprint address

Prof. H.-J. Kull, Institut für Theoretische Physik A,

RWTH Aachen, Templergraben 55, 52056 Aachen, Germany

E-Mail: kull@ilt.fhg.de, Phone: +49-241-8906-182, FAX: +49-241-80-22188

Short title

Clusters in intense laser fields

Manuscript

Pages: 1-23, Figures: 1-9

2d-PIC simulation of atomic clusters in intense laser fields

Abstract

Collective absorption of intense laser pulses by atomic clusters is studied by PIC simulations. The cluster is modelled in two-dimensional calculations as a cylindrical plasma column with a diameter of $D = 6.4$ nm and an initial electron density of $n_{e0} = 10^{23}$ cm^{-3}. The frequency and intensity dependence of absorption is discussed. It is found that non-resonant absorption by electron emission increases as a power law with the laser intensity. The absorbed energy per electron reaches a maximum of about $W_{max} = m\omega_p^2 D^2$ (ω_p: plasma frequency, m: electron mass) at the intensity where ionization saturates.

Keywords: Plasma simulation, Particle-in-cell method, Atomic clusters, Intense laser fields, Laser light absorption in plasmas

I. INTRODUCTION

In the past years the interaction of intense laser pulses with atomic clusters has received special attention. The specific absorption properties of atomic clusters (Ditmire *et al.* (1997a)) provide an efficient transfer of energy from the laser pulse to electrons and ions (Ditmire *et al.* (1998, 1997b); Shao *et al.* (1996)). Subsequent collision processes can triggger further atomic and nuclear reactions. Hard x-rays from inner-shell transitions (Ditmire *et al.* (1995); McPherson *et al.* (1994)) and high neutron yields from fusion reactions in DT clusters (Ditmire *et al.* (1999)) have been observed. A survey of recent developments in this field has been presented by Posthumus (2001).

The effective heating of large atomic clusters has been attributed partly to collisional absorption and partly to resonance absorption. A plasma model of heating has been developed including ionization rates, collision rates and hydrodynamic motion (Ditmire *et al.* (1996)). Particle simulations of small clusters have also been reported (Ditmire (1998)). In the present work, we wish to study collective absorption of a nano-plasma in the framework of particle-in-cell (PIC) simulations. This approach does not include atomic ionization and collisions but it can more fully account for collective absorption including resonance absorption and absorption by electron emission into vacuum (Brunel (1987)). We have performed various simulations in one, two and three dimensions assuming plane, cylindrical and spherical cluster geometries. Here we will present results for a cylindrical plasma column which we have obtained by relativistic electromagnetic PIC simulations in two dimensions. This work is an extension of a previous 1d electrostatic analysis of a thin plasma layer (Greschik *et al.* (2000)). Recently we have also accomplished calculations of 3d spherical plasmas which represent the actual geometry of clusters. These results will be presented in detail elsewhere.

One of the major differences between atoms and clusters in strong fields is a quite different intensity dependence. A single-electron atom has a relatively sharp optical field ionization threshold. In contrast, for atomic clusters there is a considerable intensity range from the threshold intensity for ionization of single atoms up to the saturation intensity for the ionization of the whole cluster. In this work we have studied the ionization degree and the absorbed energy of clusters in the complete range of laser intensities. It is found that the number of free electrons increases approximately linearly with the laser field and

the absorbed energy follows a simple power law up to a maximum energy where collective absorption saturates. However, the intensity scaling of the absorbed energy depends on the geometry and it therefore cannot be predicted by previous one-dimensional capacitor models (Bonnaud *et al.* (1991); Brunel (1987); Greschik *et al.* (2000)).

II. THERMAL EQUILIBRIUM

We first describe the equilibrium state that is reached after the electrons of a cylindrical plasma have been heated up to temperature T. We assume that the electrons reach equilibrium while the ions are still cold and uniformly distributed within a cylinder. This idealized equilibrium model can give some insight into the role of the Debye length in a finite size plasma, the magnitude of the surface electric field and into the maximum energy that can be absorbed by the cluster.

The electrostatic potential ϕ produced by the electron density n_e and the ion density n_i is determined by solving Poisson's equation

$$\Delta\phi = -4\pi q_e(n_e - Zn_i) \tag{1}$$

with

$$n_e \;=\; n_{e0}\exp\left(-\frac{q_e\phi}{T}\right), \qquad n_i = n_{i0}\Theta(R-r), \tag{2}$$

respectively. Here R denotes the radius of the ion density and Z the ion charge state. Looking for cylindrically symmetric solutions of (1) yields

$$y''(x) + \frac{1}{x}y'(x) + qe^{-y(x)} \;=\; \Theta(p-x) \tag{3}$$

with the dimensionless variables,

$$y = \frac{q_e\Phi}{T}, \qquad x = \frac{r}{\lambda_D}, \qquad p = \frac{R}{\lambda_D}, \qquad q = \frac{n_{e0}}{Zn_{i0}},$$

and the Debye length of the electrons

$$\lambda_D = \sqrt{\frac{T}{4\pi q_e^2 n_{e0}}}.$$

The differential equation (3) has to be supplemented by appropriate boundary conditions. Here it will be assumed that there is no charge singularity at the origin and that the total

charge of the plasma is zero,

$$\lim_{R\to 0} \int_0^R (n_e - Zn_i)\, r dr = 0$$
$$\lim_{R\to \infty} \int_0^R (n_e - Zn_i)\, r dr = 0,$$

respectively. These conditions can be expressed by the boundary conditions,

$$y'(0) = 0, \qquad y'(\infty) = 0,$$

for the electric field $y'(x)$. In the absence of a charge singularity, the potential remains finite at the origin and $y(0) = 0$ can be chosen without loss of generality. This choice defines the constant n_{e0} in Eq.(2) to be the electron density on the axis.

The boundary conditions can only be met for a specific value of the parameter q, which determines the central density n_{e0}. We have numerically integrated the differential equation with the starting values $y(0) = 0$ and $y'(0) = 0$ at the center. The parameter q then was adjusted to achieve convergence at infinity. The results are presented in Fig.1. The typical behaviour of these solutions depends on the ratio $p = R/\lambda_D$ of the radius of the column over the Debye length of the electrons. For $p \gg 1$ the column is neutralized in the center and the electric field is localized near the surface, reaching a maximum value close to $T/|q_e|\lambda_D$. When the cluster radius is reduced to the order of the Debye length, screening of the positive charge is no longer effective and the field approaches the field produced by the ions. For $p < 2$ the electrons are no longer bound by the ions and no equilibrium exists. This may be seen by noting that the number of electrons has to remain finite according to charge neutrality. The unscreened ion potential outside of the column is given by

$$y = \frac{p^2}{4} + \frac{p^2}{2} \ln\left(\frac{x}{p}\right). \tag{4}$$

Since the actual potential will be less attractive, a necessary requirement for an equilibrium to exist is that the electron number given by the unscreened potential (4) remains finite,

$$\int_R^\infty n_e r dr \propto \int_R^\infty \exp\left(-\frac{p^2}{2}\ln r\right) r dr = \int_R^\infty \frac{1}{r^{\frac{p^2}{2}-1}} dr < \infty. \tag{5}$$

This integral will only converge if $p^2/2 - 1 > 1$ or $p > 2$. In accordance with this criterium we could not find convergence of the numerical solution for the case $p = 1$.

As the cluster is heated its Debye length increases. The maximum temperature of a bound equilibrium state, corresponding to the condition $p = 2$, is given by

$$T = \frac{1}{4} m \omega_p^2 R^2, \qquad \omega_p^2 = \frac{4\pi q_e^2 n_{e0}}{m} \tag{6}$$

where ω_p denotes the plasma frequency and m_e the electron mass. Above this temperature, the electrons will be basically free and absorption can be expected to saturate in the collisionless limit. The following calculations indicate that the maximum absorbed energy per particle shows the same scaling, being of the order of $m\omega_p^2 D^2$, where $D = 2R$ is the diameter of the column.

III. PIC-SIMULATION

To gain a better understanding of collective absorption in clusters we have performed PIC simulations for a plasma column in an intense laser field. It is assumed that the atoms of the cluster are ionized nearly instantaneously and homogeneously to some charge state Z. The initial densities of electrons and ions are taken as $n_{e0} = Z n_{i0} = 10^{23}$ cm^{-3}, respectively, within a cylinder of radius $R = 3.2$ nm. Neglecting the ionization energy in comparison with the ponderomotive potential of the laser field, the particles are distributed at rest and the motion of the electrons is calculated in the mean-field approximation by the PIC method. The ions are treated as immobile. The present simulations focus on the collective dynamics of free electrons neglecting atomic processes as well as collisions.

The magnetic field of the incident laser pulse is oriented along the cylinder axis. The motion of the electrons takes place in a plane perpendicular to the cylinder axis. It is treated by relativistic electromagnetic 2d2v PIC simulations based on the methods of Birdsall and Langdon (1991). We use $16 - 64$ particles per cell and $128 - 2048$ cells per coordinate. The laser pulse is modelled as a $\sin^2$-pulse with eight cycles in most calculations. We have varied the frequency of the laser between $\omega = (0.05 - 1.3)\omega_p$ to distinghuish between non-resonant absorption of an overdense plasma and resonant absorption near the plasma frequency. The intensity has been varied in the range $10^{13} - 10^{19}$ W/cm^2 which starts at the threshold intensity for electron emission and extends up to the saturation intensity for complete ionization of the cluster. Some of the results are summarized in the following sections.

Non-resonant absorption at low frequencies and high intensities is mainly determined by electrons emitted from the cluster. Within the cluster the electrons are in a quasistatic equilibrium between the external laser field and the electrostatic restoring force of the ions. Far from the cluster electrons are oscillating in the the laser field. Crossing of the surface of the cluster introduces some phaseshift with respect to the quiver motion of free electrons that is responsible for energy gain. As a measure of the number of electrons emitted from the cluster we define an ionization degree of the cluster in the following manner. At the end of the laser pulse the fraction of electrons exterior to the ion cylinder is determined as a function of time and averaged over one further light period in the absence of the field. After the pulse, the number of emitted electrons varies only slightly due to electrons leaving or entering the cylinder and its average is a rather well-defined quantity in simulations. However it is noted, that this definition is different from the experimentally accessible charge states of single ions or the theoretical ionization degree of atoms in thermal equilibrium.

A. Threshold intensity

First, we will discuss the plasma response at the intensity $I = 10^{14}$ W/cm^2, which is close to the typical threshold intensities for tunneling ionization (Görlinger *et al.*, 2000),

$$I_{th} = \frac{Z^6}{256}\, I_{at}, \qquad I_{at} = 3 \times 10^{16}\mathrm{W/cm}^2.$$

The intensity I_{at} denotes the intensity that corresponds to a field strength of one atomic unit. In the present simulations, atomic ionization is not included, but the binding potential due to the positive charge of the total cluster leads to a more gradual increase in the number of emitted electrons. At an intensity of $I = 10^{14}$ W/cm^2 a typical fraction of a few percent of the electrons has been emitted.

In Fig.2, one can recognize the evolution of the charge density for two different laser pulses. The first pulse has a frequency $\omega = 0.1\omega_p$ and a pulse duration of 8 periods. The second pulse has a frequency $\omega = \omega_p$ and a pulse duration of 64 periods. For comparison, the resonance frequency of a cylindrical plasma column is given by

$$\frac{\omega_p}{\sqrt{2}} = 0.707\omega_p. \tag{7}$$

In the first case the quiver amplitudes of the electrons are much larger and one can recognize the acceleration of electrons emitted into vacuum. These electrons are first removed from

a surface layer while the interior region remains neutral. Later, the interior of the cluster is also heated. In the second case, the quiver amplitudes on the vacuum side are reduced. The density distribution shows a more spherically symmetric shape with small superimposed dipole oscillations.

The frequency dependence of the absorbed energy is shown in Fig.3. In varying the frequency the pulse duration and therefore also the pulse energy was kept constant. The absorbed energy is defined by the difference between the total energies per particle before and after the laser pulse. It is expressed in units of $m\omega_p^2 D^2$. The figure shows a clear resonance peak at the resonance frequency (7) of a cylindrical plasma column. The figure also shows the ionization degree as defined above, which has a similar resonance behavior. For non-resonant excitation only a few percent of electrons leave the cluster.

B. Saturation intensity

With increasing intensity the fraction of emitted electrons plays a more dominant role until all electrons are removed from the cluster at the saturation intensity. We have plotted corresponding results for an intensity of $I = 10^{17}$ W/cm^2, which is somewhat below the saturation intensity. Looking at the charge density distribution in Fig.4 one can no longer see major differences between excitations below and above the resonance frequency. In both cases more than 50% of the electrons have been emitted into vacuum in the final stage.

The absorbed energy has also a different frequency dependence as can be seen in Fig.5. The resonance maximum is somewhat shifted to lower frequencies and its width is strongly broadened. This effect is to be expected since electrons that oscillate across the cluster surface experience a reduced restoring force on the vacuum side. On the average, this reduction will lead to lower oscillation frequencies. It can further be seen that absorption now increases towards lower frequencies. Non-resonant absorption at low frequencies can even be larger than resonance absorption. This non-resonant absorption is attributed to electrons emitted into vacuum. These electrons gain energies of the order of the quiver energy in the laser field. The quiver velocity $v = qE/m\omega$ increases with decreasing frequency. The fraction of emitted electrons shows a smooth variation in the frequency range considered.

It is also interesting to note, that the charge density patterns indicate the presence of harmonics of the laser frequency. These can most easily be recognized in Fig.4 for the smaller

frequency $\omega = 0.1\omega_p$, being well separated from the plasma resonance. After one period of the laser the density shows three wavetrains excited by the third harmonic. Actually, the dipole spectrum shows maxima at the fundamental, at the third harmonic and at the column resonance (Fig.6).

C. Intensity scaling

For non-resonant absorption by electrons emitted into vacuum one expects a simple scaling of the absorbed energy with the laser intensity. The number of emitted electrons N_{free} is determined by the displacement ξ of the electrons in the cluster. Assuming a linear restoring force within the cluster one has $N \propto \xi \propto E$. The energy W_{free} gained by each emitted electron may be assumed to be some fraction of the quiver energy which is proportional to E^2. Based on these assumptions the absorbed energy will scale with the laser intensity $I \propto E^2$ as

$$W_{abs} \propto I^{3/2}. \tag{8}$$

This scaling law was originally proposed by Brunel (1987).

In the framework of the present PIC simulations of a cylindrical plasma column, we have studied the intensity scaling of non-resonant absorption. For these calculations an 8-cycle $\sin^2$-pulse with a frequency of $\omega = 0.1\omega_p$ has been used. The results are presented in Fig.7. In an intensity range between 10^{14} and 10^{18} W/cm^2 the absorbed energy obeys to a good approximation a power law

$$W_{abs} \propto I^{1.3}. \tag{9}$$

The exponent is larger than 1, corresponding to linear optics, but it is also somewhat smaller than the value 1.5 of Eq.(8). We note that this scaling law is not very sensitive to variations of the frequency between $0.1\omega_p$ and $0.07\omega_p$ or to variations of the particle numbers between 12868 and 3217. Differences between these cases can only be observed for intensities below 10^{14} W/cm^2.

The discrepancy between the observed scaling (9) and the estimate (8) has the following origin. The fraction of emitted electrons as a function of the laser intensity is shown in Fig.8. One can recognize a gradual increase of the ionization degree around 10^{14} W/cm^2 up to the saturation around 10^{18} W/cm^2. In the intermediate intensity regime the fraction of emitted electrons increases roughly linearly with the laser field, as indicated by the solid line. The

scaling $N_{free} \propto E$ therefore is satisfied to a reasonable approximation. The average energy per particle in units of the ponderomotive potential

$$U_p = \frac{m}{4}\left(\frac{qE}{m\omega}\right)^2 \tag{10}$$

is represented in Fig.9. The total energy increases up to a maximum around 10^{18} W/cm^2. The partition of the total energy into kinetic and potential energies is also shown. It indicates that the potential energy also makes a significant contribution. Finally, one can see the average kinetic energy of the emitted electrons. These energies rise up to a broad plateau of about $0.5U_p$ but then decrease again towards higher intensities. The absorption efficiency of emitted electrons obviously decreases as one approaches the saturation intensity and the kinetic energy of the emitted electrons is no longer a constant fraction of the ponderomotive potential.

IV. CONCLUSIONS

The interaction of atomic clusters with intense laser pulses has been modelled by 2d2v-PIC simulations. The code treats the interaction fully electromagnetic and relativistic but at present it is limited to two dimensions. In this framework collective absorption of a cylindrical plasma column has been analyzed. It is found that resonance absorption occurs near the resonance frequency of the cylindrical plasma column at moderate laser intensities. At higher intensities the resonance is strongly broadened and in addition there is significant non-resonant absorption by electrons emitted into vacuum. Above the ionization threshold, the fraction of emitted electrons scales roughly linearly with the electric field. The absorption efficiency of free electrons, defined as the fraction of ponderomotive energy gained by these electrons, shows a more complicated behaviour and decreases strongly towards the saturation intensity. As a result the intensity scaling of non-resonant absorption is different from the one-dimensional case. The maximum energy absorbed per particle by a single cluster with diameter D and plasma frequency ω_p is about $W_{max} = m\omega_p^2 D^2$. This energy is gained when the intensity reaches or exceeds the saturation intensity.

Presently our calculations are extended to three-dimensional spherical clusters. For this purpose it is found advantageous to use particle simulations with a regularized Coulomb-interaction at small distances. This method avoids large numerical grids in PIC simulations

and proves sufficient to deal with the long-range collective interaction. It is found that the intensity scaling in the three-dimensional case is further reduced.

Another extension of the present model concerns the inclusion of ion motion. As the cluster expands its density varies from overcritical to undercritical. At the critical density strong resonance absorption can be observed. The particle simulations with ion motion indicate, that the plasma resonance can actually be reached after about 35 laser periods for an intensity of 10^{14} W/cm^2. These and other results of the spherical system will be treated in a forthcoming paper.

Acknowledgments

The authors are grateful to B.U. Felderhof, R. Schmitz and P. Mulser for discussions.

References

Birdsall, C. K., and A. B. Langdon (1991). *Plasma Physics via Computer Simulation*. Bristol and Philadelphia: IOP Publishing.

Bonnaud, G., P. Gibbon, J. Kindel, and E. Williams (1991). Laser and Particle Beams **9**, 339-354.

Brunel, F. (1987). Phys. Rev. Lett. **59**, 52-55.

Ditmire, T. (1998). Phys. Rev. A **57**, R4094-R4097.

Ditmire, T., T. Donnelly, R. W. Falcone, and M. D. Perry (1995). Phys. Rev. Lett. **75**, 3122-3125.

Ditmire, T., T. Donnelly, A. M. Rubenchik, R. W. Falcone, and M. D. Perry (1996). Phys. Rev. A **53**, 3379-3402.

Ditmire, T., R. A. Smith, J. W. G. Tisch, and M. H. R. Hutchinson (1997)a. Phys. Rev. Lett. **78**, 3121-3124.

Ditmire, T., E. Springate, J. W. G. Tisch, Y. L. Shao, M. B. Mason, N. Hay, J. P. Marangos, and M. H. R. Hutchinson (1998). Phys. Rev. A **57**, 369-382.

Ditmire, T., J. W. G. Tisch, E. Springate, M. B. Mason, N. Hay, R. A. Smith, J. Marangos, and M. H. R. Hutchinson (1997)b. Nature (London) **386**, 54-56.

Ditmire, T., J. Zweiback, V. P. Yanovsky, T. E. Cowan, G. Hays, and K. B. Wharton (1999). Nature **398**, 489-492.

Görlinger, J., L. Plagne, and H.-J. Kull (2000). Appl. Phys. B **71**, 331-336.

Greschik, F., L. Dimou, and H.-J. Kull (2000). Laser and Particle Beams **18**, 367-373.

McPherson, A., B. D. Thompson, A. B. Borisov, K. Boyer, and C. Rhodes (1994). Nature(London) **370**, 631-634.

Posthumus, J. (2001). *Molecules and Clusters in Intense Fields*. The Edinburgh Building, Cambridge CB2 2RU, UK: Cambridge University Press.

Shao, Y. L., T. Ditmire, J. W. G. Tisch, E. Springate, J. P. Marangos, and M. H. R. Hutchinson (1996). Phys. Rev. Lett. **77**, 3343-3346.

FIGURE CAPTIONS

Fig.1 Thermal equilibrium of a cylindrical plasma column of radius R. a)-c) If the radius is much larger than the Debye length λ_D the electrons neutralize the interior of the column. The surface field is determined by $eE\lambda_D \approx T$. d) If $R < 2\lambda_D$ the ion field E_i can no longer be screened by electrons and no bound equilibrium exists.

Fig.2 Charge density excitations below ($\omega = 0.1\omega_p$) and above ($\omega = 1.0\omega_p$) the resonance frequency ($\omega_p/\sqrt{2}$) of a cylindrical cluster at an intensity of 10^{14} W/cm^2 (D_0: cylinder diameter, T_0: laser period).

Fig.3 Absorbed energy W_{abs} and fraction of emitted electrons g as a function of the laser frequency for $I = 10^{14}$ W/cm^2. The maximum corresponds to the resonance of a cylindrical plasma column at the frequency given by Eq.(7).

Fig.4 Charge density excitations below ($\omega = 0.1\omega_p$) and above ($\omega = 1.0\omega_p$) the resonance frequency ($\omega_p/\sqrt{2}$) of a cylindrical cluster at an intensity of 10^{17} W/cm^2 (D_0: cylinder diameter, T_0: laser period).

Fig.5 Absorbed energy W_{abs} and fraction of emitted electrons g as a function of the laser frequency for $I = 10^{17}$ W/cm^2. In addition to a broad resonance peak one observes significant absorption at low frequencies due to electrons that are emitted and subsequently accelerated by the laser field. The quiver energy of these electrons increases with decreasing frequency.

Fig.6 Power spectrum of the x- and y-components of the dipol moment for $\omega = 0.1\omega_p$ (left) and $\omega = \omega_p$ (right) at $I = 10^{17}$ W/cm^2. There are peaks at the laser frequency and at the plasma resonance frequency. For $\omega = 0.1\omega_p$ one can observe in addition odd harmonics in the y-component and even harmonics in the x-component.

Fig.7 Absorbed energy W_{abs} per particle as a function of the laser intensity. Solid squares indicate the data for the frequency $\omega = 0.1\omega_p$. For the intensity range $10^{14} < I < 10^{18}$ W/cm^2 absorption is dominated by electron emission and a scaling $\propto I^{1.3}$ can be found. The absorption of bound electrons at smaller intensities shows a scaling $\propto I$ but its magnitude depends on the details of the model (frequency, number of simulation particles J).

Fig.8 Ionization degree, defined as the fraction of emitted electrons, as a function of the laser intensity. One can recognize a gradual increase at around 10^{14} W/cm^2 and saturation at about 10^{18} W/cm^2. For intermediate intensities the number of emitted particles increases approximately linearly with the electric field $E \propto \sqrt{I}$.

Fig.9 Energies per particle in units of the ponderomotive potential $U_p = m(qE)^2/(2m\omega)^2$ as a function of the laser intensity.

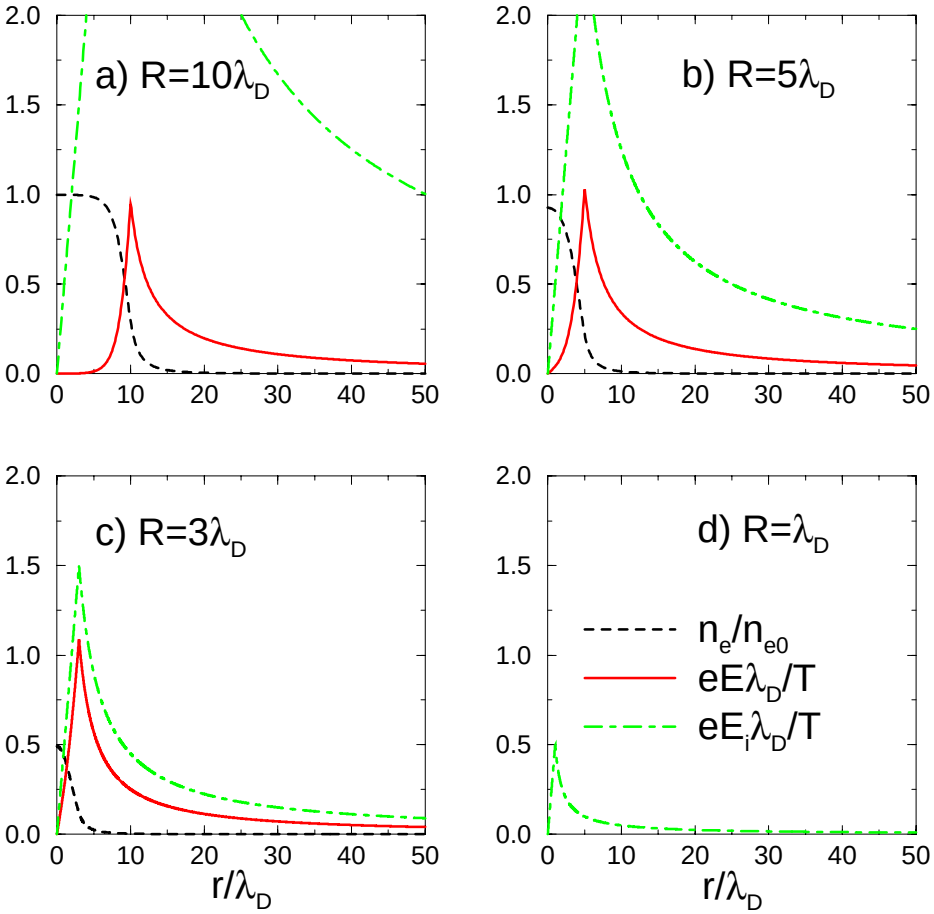

FIG. 1 Thermal equilibrium of a cylindrical plasma column of radius R. a)-c) If the radius is much larger than the Debye length λ_D the electrons neutralize the interior of the column. The surface field is determined by $eE\lambda_D \approx T$. d) If $R < 2\lambda_D$ the ion field E_i can no longer be screened by electrons and no bound equilibrium exists.

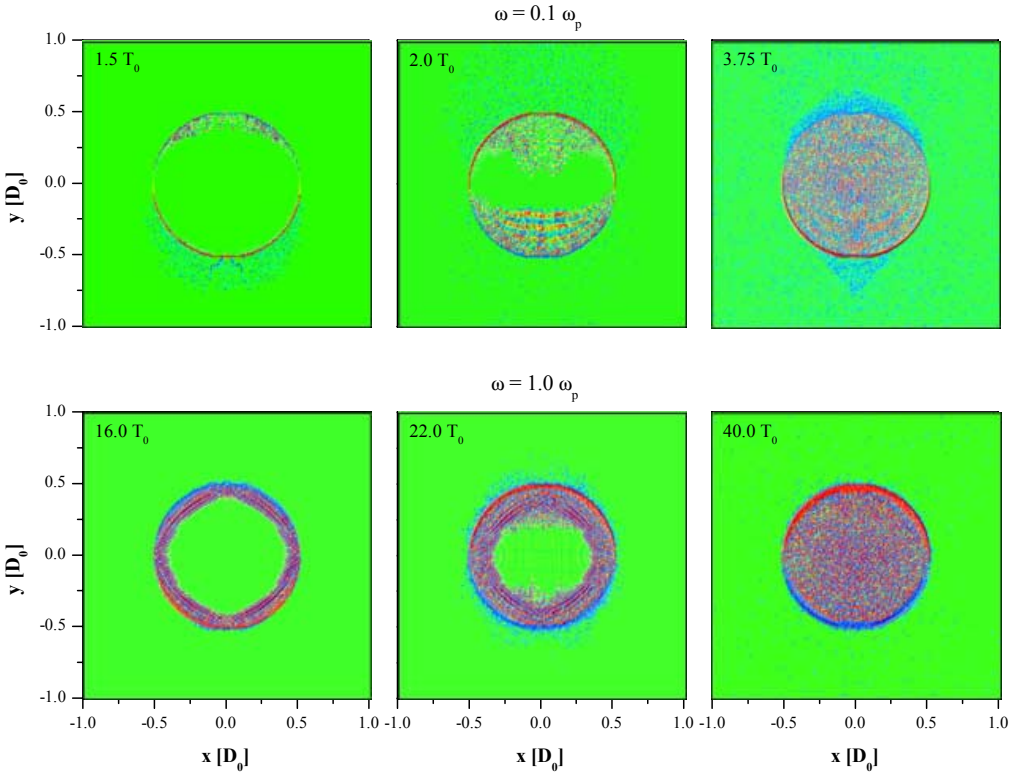

FIG. 2 Charge density excitations below ($\omega = 0.1\omega_p$) and above ($\omega = 1.0\omega_p$) the resonance frequency ($\omega_p/\sqrt{2}$) of a cylindrical cluster at an intensity of 10^{14} W/cm^2 (D_0: cylinder diameter, T_0: laser period).

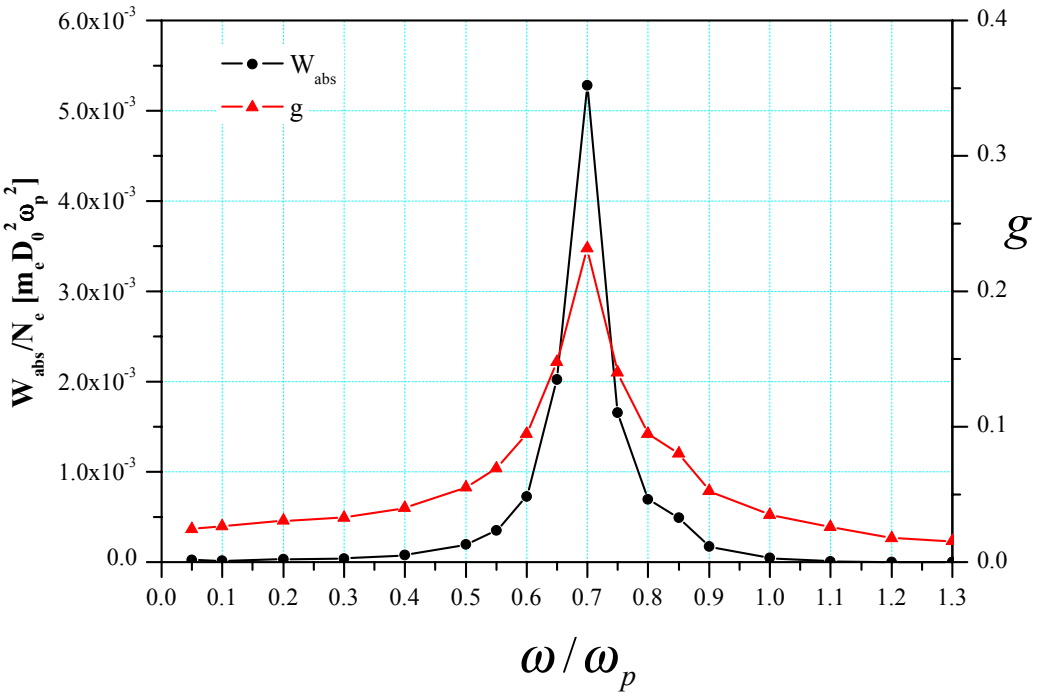

FIG. 3 Absorbed energy W_{abs} and fraction of emitted electrons g as a function of the laser frequency for $I = 10^{14}$ W/cm^2. The maximum corresponds to the resonance of a cylindrical plasma column at the frequency given by Eq.(7).

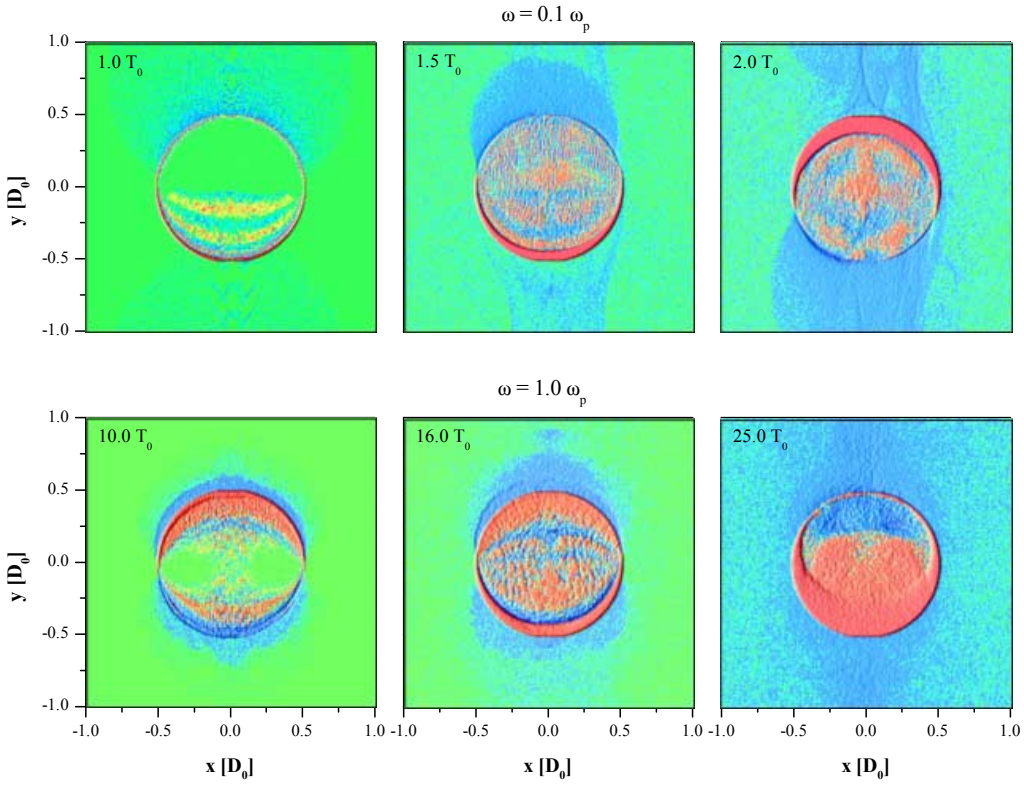

FIG. 4 Charge density excitations below ($\omega = 0.1\omega_p$) and above ($\omega = 1.0\omega_p$) the resonance frequency ($\omega_p/\sqrt{2}$) of a cylindrical cluster at an intensity of 10^{17} W/cm^2 (D_0: cylinder diameter, T_0: laser period).

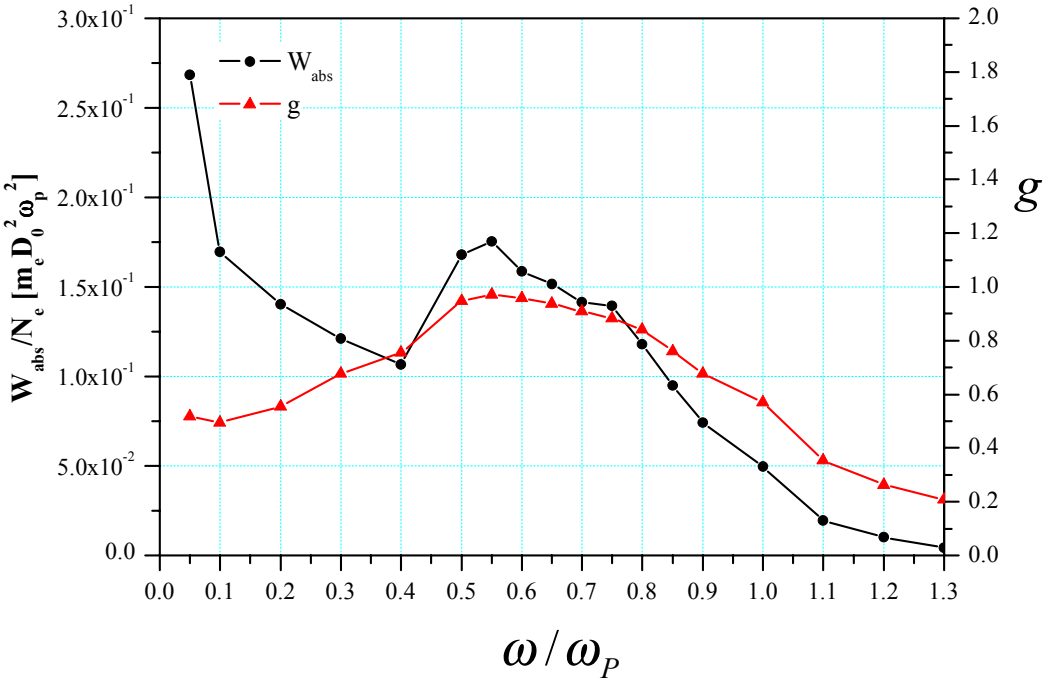

FIG. 5 Absorbed energy W_{abs} and fraction of emitted electrons g as a function of the laser frequency for $I = 10^{17}$ W/cm^2. In addition to a broad resonance peak one observes significant absorption at low frequencies due to electrons that are emitted and subsequently accelerated by the laser field. The quiver energy of these electrons increases with decreasing frequency.

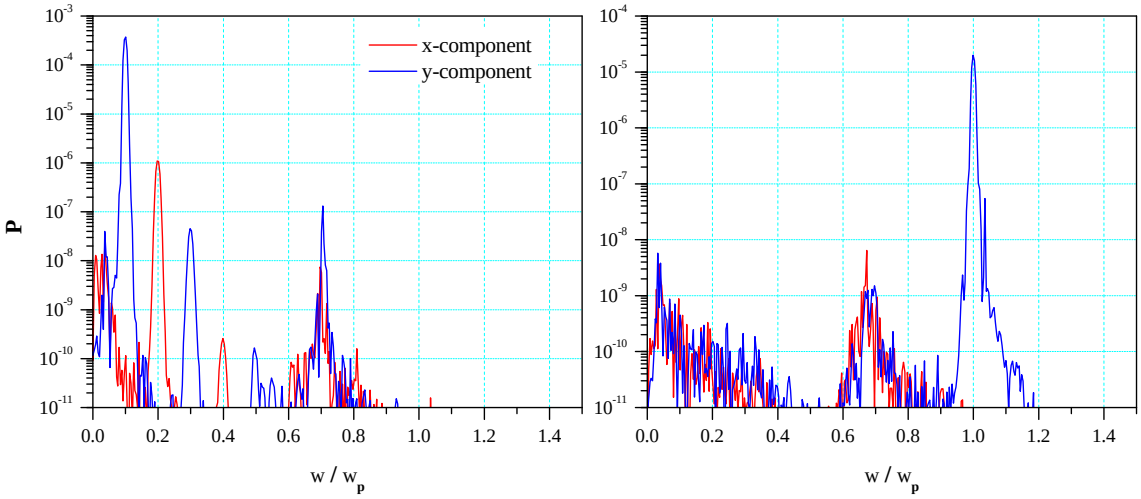

FIG. 6 Power spectrum of the x- and y-components of the dipol moment for $\omega = 0.1\omega_p$ (left) and $\omega = \omega_p$ (right) at $I = 10^{17}$ W/cm^2. There are peaks at the laser frequency and at the plasma resonance frequency. For $\omega = 0.1\omega_p$ one can observe in addition odd harmonics in the y-component and even harmonics in the x-component.

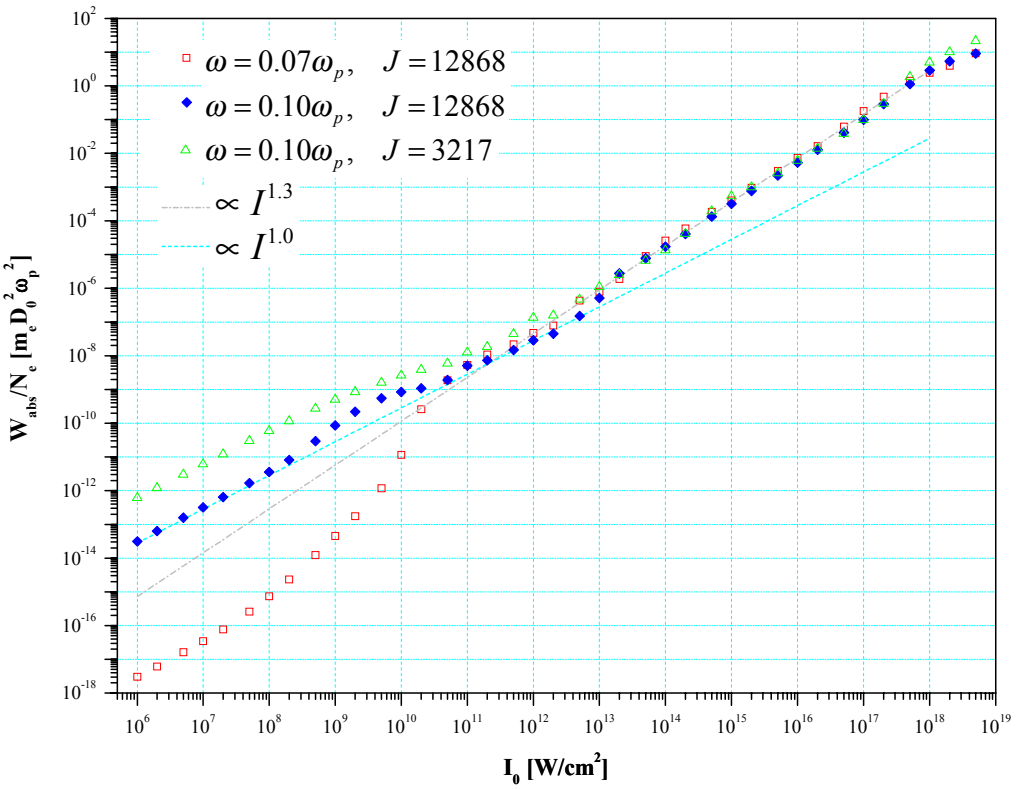

FIG. 7 Absorbed energy W_{abs} per particle as a function of the laser intensity. Solid squares indicate the data for the frequency $\omega = 0.1\omega_p$. For the intensity range $10^{14} < I < 10^{18}$ W/cm^2 absorption is dominated by electron emission and a scaling $\propto I^{1.3}$ can be found. The absorption of bound electrons at smaller intensities shows a scaling $\propto I$ but its magnitude depends on the details of the model (frequency, number of simulation particles J).

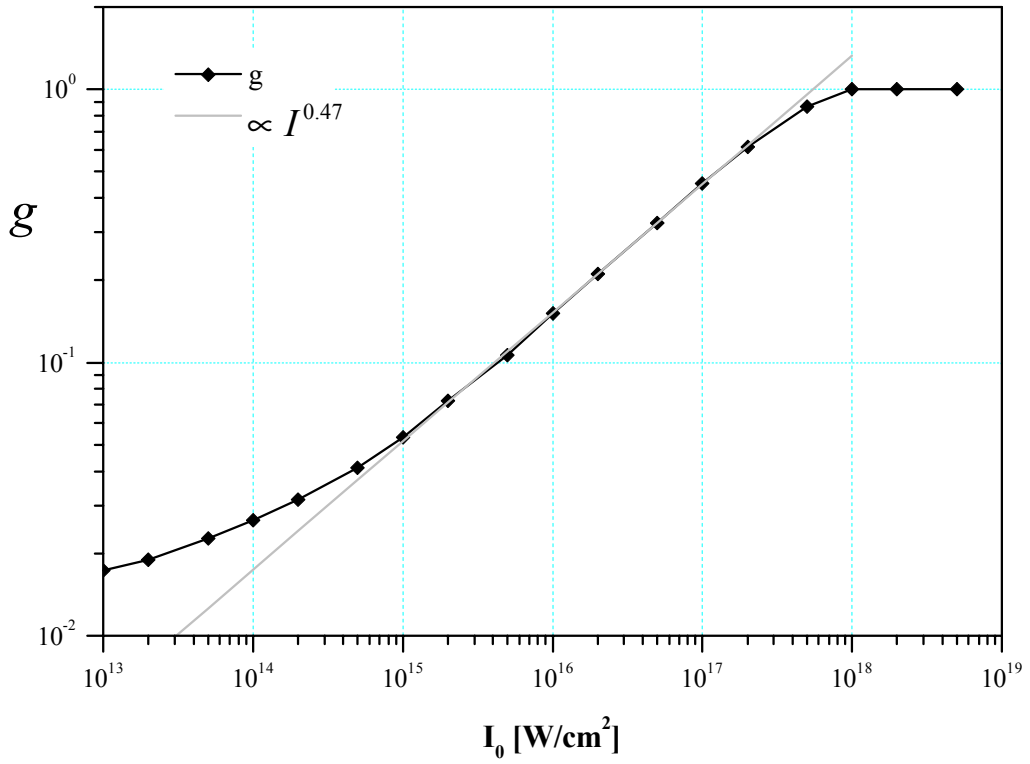

FIG. 8 Ionization degree, defined as the fraction of emitted electrons, as a function of the laser intensity. One can recognize a gradual increase at around 10^{14} W/cm^2 and saturation at about 10^{18} W/cm^2. For intermediate intensities the number of emitted particles increases approximately linearly with the electric field $E \propto \sqrt{I}$.

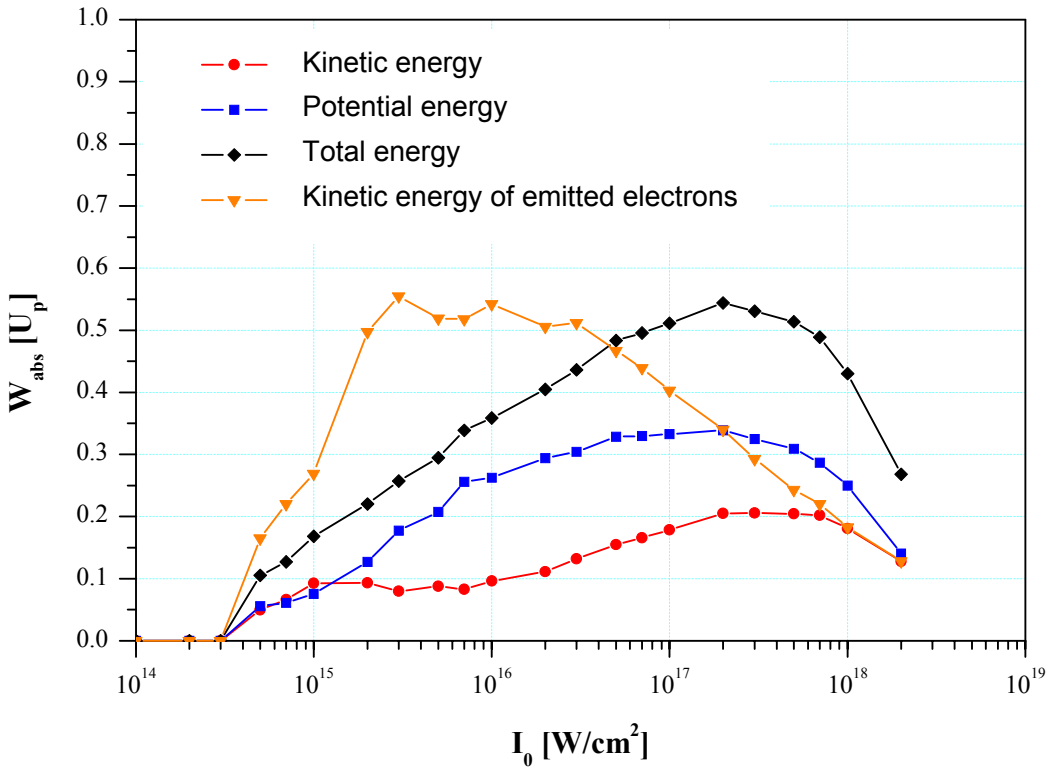

FIG. 9 Energies per particle in units of the ponderomotive potential $U_p = m(qE)^2/(2m\omega)^2$ as a function of the laser intensity.